FATIGUE CRACK INITIATION AND PROPAGATION IN CHROMIUM PRE-ALLOYED PM STEELS

R. Gerosa[1], B. Rivolta[1], A. Tavasci[1], G. Silva[1]

[1] Politecnico di Milano, Polo Regionale di Lecco, Italy

ABSTRACT.
Powder metallurgy processing of steels typically results in a material characterized by residual porosity, whose dimension and morphology, together with the microstructure, strongly affect the fatigue crack growth behaviour of the material. Prismatic specimens were pressed at 7.0 g/cm^3 density from Astaloy CrM powder and sintered in different conditions, varying the sintering temperature and the cooling rate after sintering. Optical observations allowed to evaluate the dimensions and the characteristics of the porosity and the microstructural characteristics for all the investigated conditions. Fatigue tests were performed at R-ratio equal to 0.1 to investigate the threshold zone and to calculate the Paris law coefficients. All the tests were carried out according with the compliance method, and the crack length has been evaluated during the whole test. Moreover K_{Ic} tests were performed in order to complete the investigation. Both on fatigue and K_{Ic} samples a fractographic analysis was carried out to investigate the crack path and the fracture surface features. The results show that the Paris law crack growth exponent is around 6.0 for 1120°C sintered and around 4.7 for 1250°C sintered materials. The same dependence to process parameters is not found for the threshold. Values close to 6 MPa√m are here found for all variants.

INTRODUCTION

The mechanical parts produced by powder metallurgy processing are characterized by some degree of residual porosity after sintering, which is known to affect the final mechanical properties of the component [1]. Moreover, the dimension and morphology of the microstructure strongly affect the fatigue crack behaviour of the steels [2-5]. The nature of porosity and the metallographic phases are influenced by several processing variables, such as the type and amount of alloying additions, the sintering temperature and time, the cooling rate after sintering or the presence of heat treatments after sintering [6-10]. In this paper fatigue tests were performed on steels from Astaloy CrM powders to investigate the threshold zone and to evaluate the Paris law, varying the sintering temperature and the cooling rate in the furnace after sintering. Moreover, K_{Ic} tests were performed to complete the investigation. The crack path and the fractographic features were investigated by optical and SEM observations and finally a

microstructural investigation was carried out on the samples sintered both at 1120°C and 1250°C.

MATERIALS CHARACTERIZATION

Three steels, obtained from AstaloyCrM powders sintered at different temperatures in hydrogen (90%) and nitrogen (10%) atmosphere, were investigated. The nominal density was 7.0 g/cm^3. In table 1 the sintering conditions are reported, while table 2 shows the chemical composition. For Cr2 and Cr3 materials a tempering at 200°C for 1 hour was carried out after sintering.

Table 1. Sintering conditions.

Material code	Sintering Temperature [°C]	Cooling rate after sintering [°C/s]
Cr1	1120	0.8
Cr2	1120	2.5
Cr3	1250	2.5

Table 2. Chemical composition of the steels.

Material code	%Cr	%Mo	% added graphite	%C after sintering
Cr1	3	0.5	0.50	0.47
Cr2	3	0.5	0.68	0.57
Cr3	3	0.5	0.68	0.62

Firstly, the dimensions and characteristics of the pores were analysed, by the calculation of porosity through an image analysis software. The materials were classified considering the area and the roundness of the pores. The total porosity was estimated equal to 10.1%. Figures 1a and 1b show the pores area distribution and the pores roundness, varying the sintering temperature. The data related to 1120°C sintering temperature refer to both Cr1 and Cr2 series, because it's known in the literature that the pores area distribution and roundness depend only on sintering temperature [6-10].

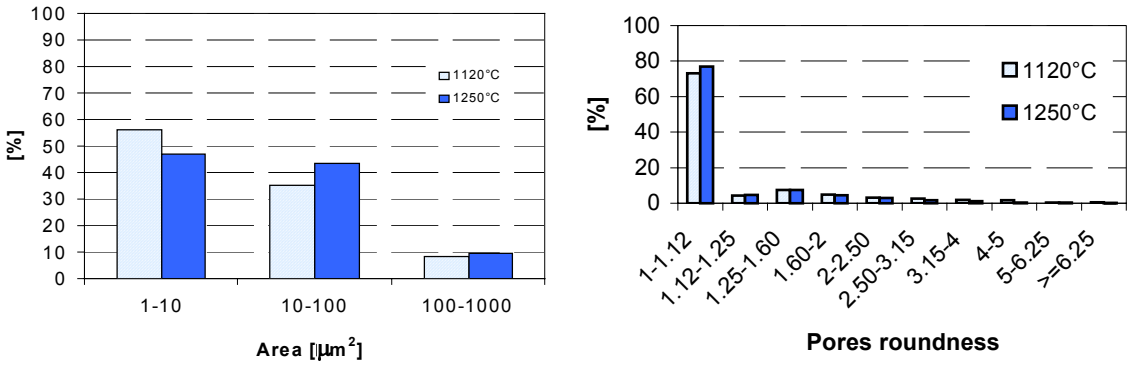

Figure 1 a): pores area distribution varying the sintering temperature; b): pores roundness varying the sintering temperature

The microstrucure and the microhardness (HV0.1) were investigated for all the materials and the obtained results are summarized in Table 3. From Figure 3 to 6 the observed metallographic phases are reported.

Table 3. Microstructure and related microhardness for Cr1, Cr2 and Cr3 steels.

	HV0.1	Microstructure		HV0.1	Microstructure		HV0.1	Microstructure
Cr1	222-237	Perlite	**Cr2**	602-634	Transforming Austenite	**Cr3**	394-560	Transforming Austenite
	397-488	Bainite		707-803	Martensite		640-707	Martensite
	649-743	Martensite						

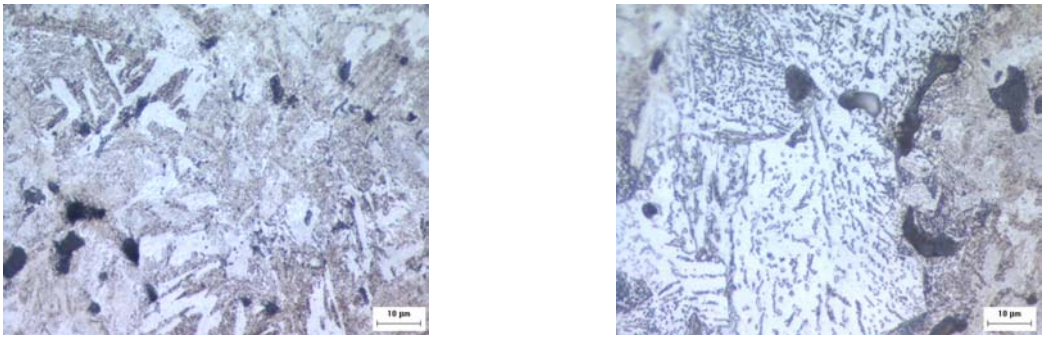

Figure 3: bainitic, martensitic and perlitic structure in Cr1 steel.

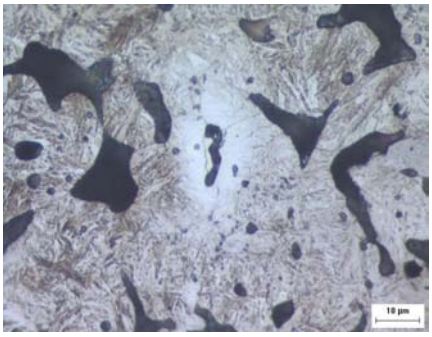

Figure 4: martensite and transforming austenite in Cr2 steel.

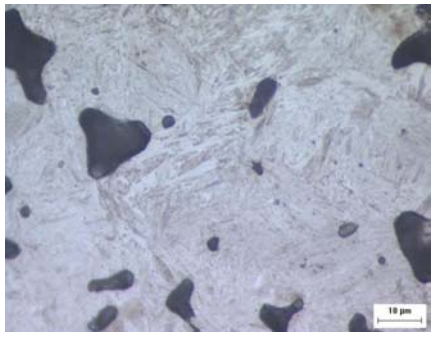

Figure 5: martensite and transforming austenite in Cr3 steel.

EXPERIMENTAL TESTS

On each series of materials, fatigue tests were performed in order to investigate the crack growth rate, both in the threshold and in the stable and unstable zones. Moreover,

K_{IC} tests were carried out to complete the investigation. Sample dimensions and precracked geometry were obtained according to the standard BS 6835 [11] for three-point single edge notch bend specimen (SENB3), while the da/dN test procedure was carried out according to the ASTM E647 standard [12]. The dimensions of the specimens are reported in Table 4.

Table 4. Specimens dimensions

*thickness **B**[mm]*	*width **W** [mm]*	*length **L** [mm]*	*span **S** [mm]*	*notch **M** [mm]*
6.40	12.08	90.00	48.32	2.60

Precracking was performed under load control, according to the compliance method: starting from an initial K value (K_{max}), the load decreases in order to give a final K (K_{min}), kept constant for a minimum crack propagation equal to 2.5% of the crack length itself. This method assures low deformation and strain-hardening at the notch tip. da/dN tests can be carried out according to two methods: the decreasing ΔK (decreasing the load) method and the increasing ΔK one (with constant load). The first series of tests aimed to calculate the Paris law and so an increasing ΔK method was performed [13]. For each material, at least three tests were carried out to confirm the validity of the results. In Figure 6 the data obtained from all the tests were represented for each series.

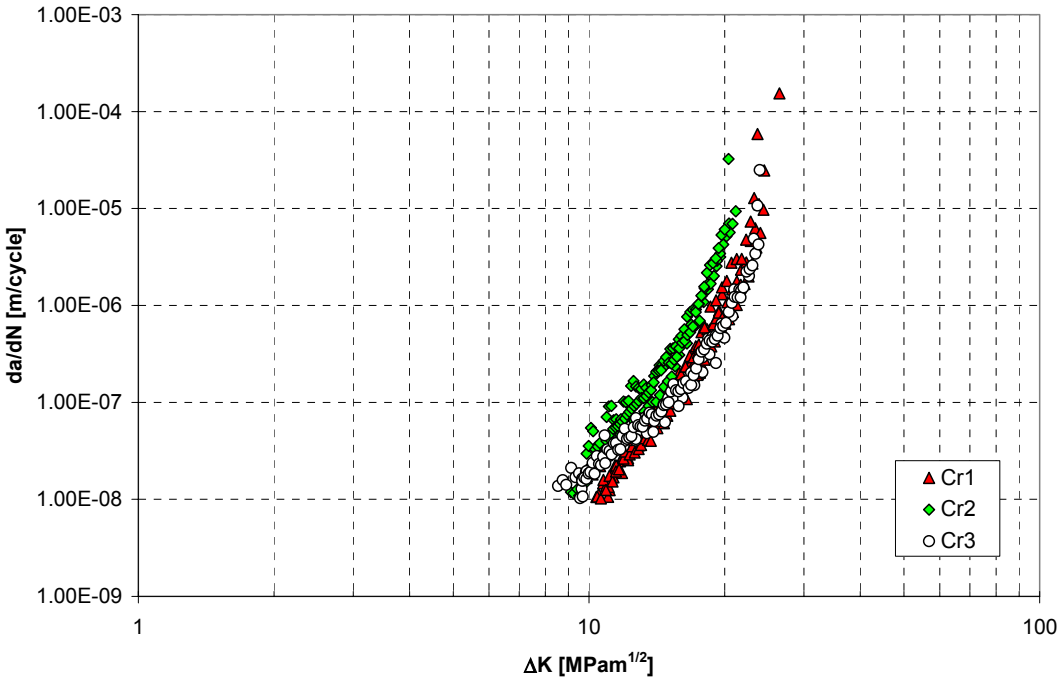

Figure 6: da/dN curves for the Cr1,Cr2 and Cr3 series, by ΔK increasing method.

From the data represented in Figure 6, the Paris law for each series was calculated between 10^{-8} and 10^{-6} m/cycle. The coefficients are reported in Table 5.

Table 5. Paris law coefficients.

Material code	C	M
Cr1	$9 \cdot 10^{-15}$	5.986
Cr2	$2 \cdot 10^{-14}$	6.066
Cr3	$4 \cdot 10^{-13}$	4.667

In the second part of this paper the investigation on the threshold zone was carried out by decreasing ΔK technique. The obtained results are summarized in Figure 7: for all the materials, crack growth rate values close to 10^{-9} m/cycle were found; only for Cr2 material, lower crach growth rate data were found.

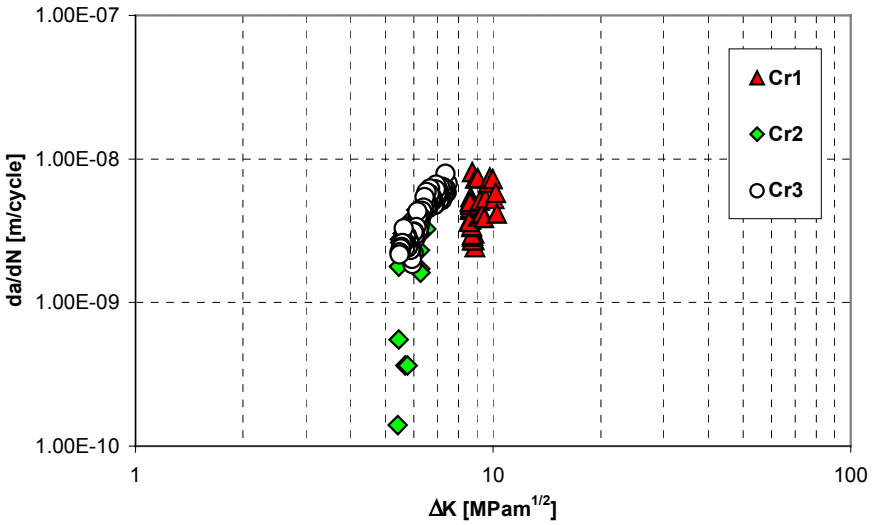

Figure 7: Threshold behaviour for the tested materials.

Microscopic observations allow the investigation of the crack path during precraking and propagation. At the notch tip, the crack nucleates from one or more pores on the free surface, as shown in Figure 8.

SEM analysis showed very interesting differences between fracture surfaces in the threshold and in the Paris zones. In the threshold zone the crack propagates both on sinter-necks and inside powder particles, without any influence of the pores characteristics or dimension, while for higher growth rates the pores seem to influence the propagation heavily, in fact the crack path tends to prefer the sinter-necks. Fracture morphology in the threshold zone appears as serrated, while in the zones where the crack speed is high and in the rupture zone, some cleavage and dimple features can be

found. This morphology has been observed in all the examined series (Figures 9-12) [14-15].

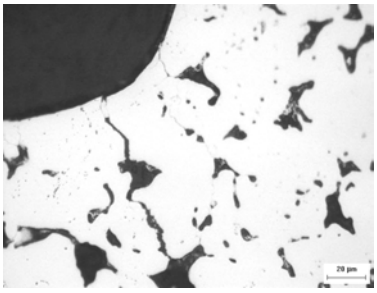

Figure 8: cracks nucleation at the notch tip.

During the test, the crack propagates through the pores and often some secondary non-propagating cracks nucleate from the pores themselves.

a) 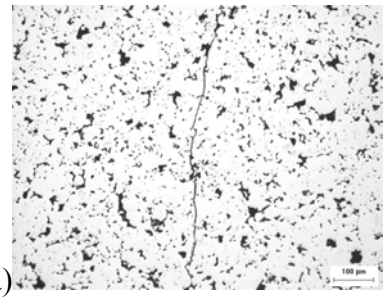 b) 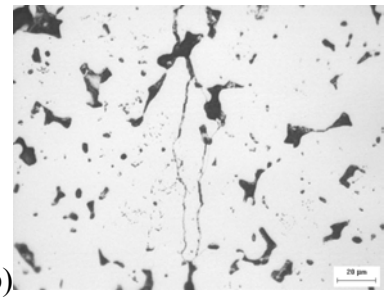

Figure 9: crack path during propagation (a) and secondary non propagating cracks (b)

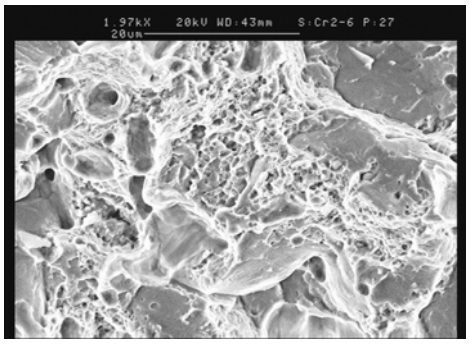

Figure 10: $da/dN \approx 10^{-7}[m/cycle]$

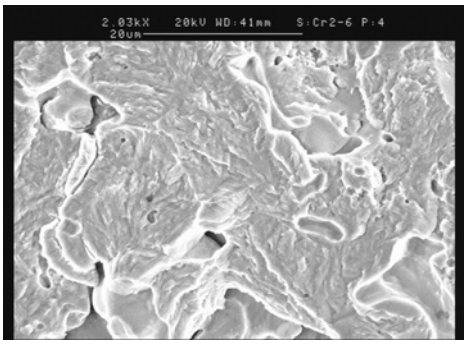

Figure 12: $da/dN \approx 3 \cdot 10^{-9}[m/cycle]$

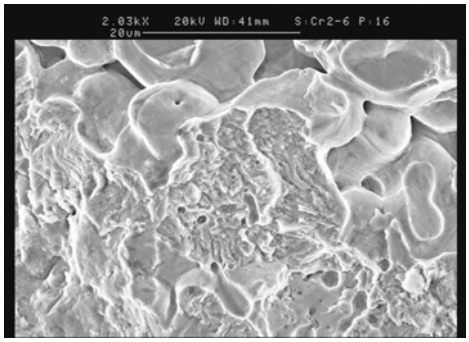

Figure 11: $da/dN \approx 5 \cdot 10^{-8} [m/cycle]$

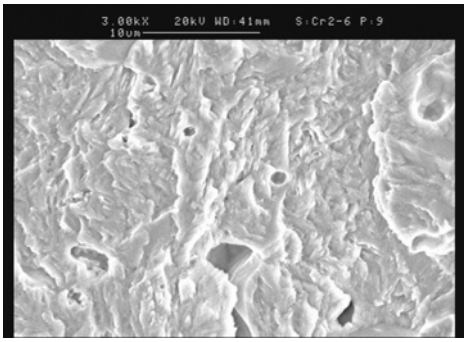

Figure 13: $da/dN \approx 2 \cdot 10^{-10} [m/cycle]$

Finally, fracture toughness tests have been performed for all the materials; the obtained results are reported in Table 6 where both K_Q and K_{Max} were reported together with the ratio P_{Max} on P_Q. Each value is evaluated as the average value between three experimental values.

Table 6. experimental values obtained from fracture toughness tests.

Material code	$K_Q[MPa\sqrt{m}]$	P_{Max}/P_Q	$K_{Max}[MPa\sqrt{m}]$
Cr1	27.0	1.14	30.8
Cr2	20.8	1.11	23.0
Cr3	26.1	1.08	28.2

From the analysis of the data, Cr1 shows both a K_Q and K_{Max} higher than Cr2 and Cr3. For Cr1 and Cr2 series, the ratio P_{Max} on P_Q is not able to respect the limit 1.1 of the ASTM E 399 Standard [16].

CONCLUDING REMARKS

In this paper, results on the effects of pores characteristics and metallographic phases on the fatigue crack initiation and propagation in Chromium pre-alloyed PM steels were reported. On the basis of these results, the following conclusions can be made

- the Paris law crack growth exponent is around 6.0 for 1120°C sintered and around 4.7 for 1250°C sintered steels
- about the steels sintered at 1120°C, observing the crack growth curve, at a given value of ΔK, the crack growth rate in Cr2 steel is higher than Cr1. This can be related to the different microstructure due to the different cooling rate from 1120°C sintering temperature: martensite and transforming austenite in Cr2 steel and perlite and martensite in Cr1. Cr1 and Cr2 steels have similar m-coefficient, but different C-coefficients of the Paris law.
- about the fatigue crack initiation, neither the pores characteristics nor metallographic phases seems to strongly influence the stress intensity threshold value.

- SEM analysis shows different features between fracture morphology in the threshold and in the Paris zones. In the threshold zone the crack propagates both on sinter-necks and inside powder particles, while for higher growth rates the pores seem to influence the propagation heavily. Fracture morphology in the threshold zone appears as serrated, while in the zones where the crack speed is high and in the rupture zone, some cleavage and dimple features can be found.

MAIN REFERENCES

1. German, R.M., Powder Metallurgy of Iron and Steel, Wiley Intersciences, New York, 1998.
2. A. Bergmark, L. Alzati, *Special Issue of Fatigue and Fracture of Engineering Materials and Structures (FFEMS),* Vol. 28, no. 1-2, 2005.
3. D.A. Gerard, D.A. Koss, Influence of porosity on short fatigue crack growth at large strain amplitudes, *Int. J. Fatigue*, Vol. 13, No. 4, 345-352, 1991.
4. Holmes J., Queeney R.A., Fatigue Crack initiation in a porous steel, *Powder Metallurgy*, v 28, n 4, p 231-235, 1985.
5. S.J. Polasik, J.J. Williams, N. Chawla, Fatigue crack initiation and propagation of binder-treated powder metallurgy steels, *Metallurgical and Materials Transactions A: Physical Metallurgy and Materials Science*, v 33, n 1, January, p 73-81, 2002.
6. G. L'Esperance, E. Duchesne, A. de Rege, Effect of Materials and Process Parameters on the Microstructure and Properties of Sinter hardening Alloys, *Advances in Powder Metallurgy & Particulate Materials*, Metal Powder Industries Federation, Princeton, NJ, 1996, 11-397/11-413.
7. G. F. Bocchini, B. Rivolta, G. Silva, P. Piccardo, M. R. Pinasco, E. Poggio, Influence of cooling rate on microstructural and mechanical properties of alloys from diffusion-bonded powders, sintered in different conditions, *P/M Science & Technology Briefs*, Vol. 4, N. 4, December 2002, 16-21.
8. G. F. Bocchini, B. Rivolta, G. Silva, M.G. Ienco, M.R. Pinasco, E. Stagno, Influence of density and surface/volume ratio on the cooling speed of sinter-hardening materials: microstructure and microhardness distribution inside parallelepipeds, *Advances in Powder Metallurgy & Particulate Materials*, Metal Powder Industries Federation, Princeton, NJ, 2002, 13-60/13-72.
9. G. F. Bocchini, B. Rivolta, G. Silva, A. Baggioli, P. Piccardo, E. Poggio, Influence of density and surface/volume ratio on the cooling speed of sinter-hardening materials: numerical analysis of parallelepipeds, *2002 World Congress on Powder Metallurgy & Particulate Materials*, Orlando, 16-21 June 2002.
10. G. F. Bocchini, A. Baggioli, R. Gerosa, B. Rivolta, G. Silva, Cooling Rates of P/M Steels, *Int. J. Powder Metallurgy*, vol.40, n.5, 2004.
11. BS 6835, Method for the determination of the rate of fatigue crack growth in metallic materials, BSI, 1998.
12. ASTM E647-00, Standard Test Method for Measurement of fatigue Crack Growth Rates, ASTM, West Conshohocken, USA
13. I. Berilsson, *Mechanical behaviour of sintered steels*, Department of Engineering Metals Chalmers University of Technology, S412 96 Goteborg, Sweden
14. H. Drar, *Transition from trans-particle to inter-particle fracture under cyclic loading of Distaloy AE + 0.5%C*, Advances in P/M & particulate materials, PM^{2}TEC 2001, New Orleans.
15. H. Drar, *Fracture mechanisms near threshold conditions of nickel alloyed PM steel*, Engineering Fracture Mechanics Vol. 55, No. 6 (1996), 901-917.
16. ASTM E 399 - 90 (Reapproved 1997), Standard test method for plane-strain fracture toughness of metallic materials, ASTM, West Conshohocken, USA

ACKNOWLEDGEMENTS

The authors gratefully acknowledge Hoganas AB, Sweden for financial support of this research.